

DOI: <https://doi.org/10.24297/jap.v16i1.8083>**Structural, Optical and Electrical Properties of MnO<sub>2</sub> / MWCNTs/PVA Nanocomposite**Safaa K. El-Mahy<sup>1</sup> and M. Dawy<sup>2</sup><sup>1</sup>Department of physics, Faculty of women for Arts, Science and Education, Ain Shams University, Cairo, Egypt.<sup>2</sup>Department of Physical Chemistry, National Research Center, Giza, 12622, Egypt.

safaa.elmahy@yahoo.com, m\_dawy9@yahoo.com

**ABSTRACT**

Manganese dioxide/multi-walled carbon nanotubes MnO<sub>2</sub>/ MWCNTs nanocomposite are synthesized by hydrothermal method. The crystallographic information of the acid-treated MWCNTs and the MnO<sub>2</sub>/ modified MWCNTs nanocomposite were characterized by X-ray diffraction (XRD), Transmission electron microscope (TEM) and FT-IR spectra. Optical and electrical properties of MnO<sub>2</sub> / MWCNTs / PVA nanocomposite thin film with different concentration were studied. UV-VIS absorption spectra shift, at different exposing time, indicated the sensitivity to UV radiation. Optical band gap decreases with increasing time of radiation. Electrical properties of MnO<sub>2</sub> / MWCNTs / PVA nanocomposite thin films with different concentration according to different frequency and exposing time of UV radiation showed semiconducting properties and sensitivity to UV radiation.

**Keywords:** MnO<sub>2</sub> / MWCNTs/ PVA nanocomposite, UV radiation, optical and electrical properties.

**1. Introduction**

Carbon nanotubes (CNTs) can be classified into single-walled carbon nanotubes (SWCNTs) and multi-walled carbon nanotubes (MWCNTs), both of which have been widely explored as an option for high power electrode materials because of their good electrical conductivity and easily accessible surface areas. Furthermore, high mechanical flexibility and open tubular network make them an ideal support for active materials. But the energy density is, however, a concern because its surface area is relatively small [1].

The shape of CNTs are a hexagonal set of carbon atoms rolled in a long, thin, hollow cylinder [2]. CNTs are hopeful materials for the electrodes of supercapacitors, due to their electrical conductivity, low mass density, high surface area and unique internal structure.

MnO<sub>2</sub> (Manganese dioxide) attracted large research care due to their characteristic physical and chemical properties and wide applications in energy storage, biosensor, ion exchange and catalysis [3-5]. MnO<sub>2</sub> has been considered as a hopeful electrode material for supercapacitors because of its low cost, environmental benignity, and excellent capacitive performance in aqueous electrolytes [6-8]. Recently, MnO<sub>2</sub> /CNTs nanocomposite has been prepared by different ways to improve the electrochemical use of MnO<sub>2</sub> and electronic conductivity of the electrode [9-12]. In recent years, supercapacitors based on MnO<sub>2</sub> as electroactive materials are attracting great attention due to the low cost of the raw material, excellent electrochemical performance and environmental compatibility [13].

The aim of the paper is to study the optical and electrical properties of MWCNTs and MnO<sub>2</sub>/ MWCNTs/ PVA nanocomposite thin film with different concentration and sensitivity to UV-radiation. MnO<sub>2</sub>/ MWCNTs / PVA nanocomposite are synthesized by hydrothermal method. MnO<sub>2</sub>/ modified MWCNTs nanocomposite characterize by XRD, TEM, FT-IR and UV-VIS. Optical and electrical properties were studied after exposing UV radiation showing the sensitivity to UV-radiation.

## 2. Experimental

### 2.1: modification of MWCNTs

MWCNTs of 1 gm supplied from (Germany) with the outer diameter of 50 nm over 1.0 m in length was dissolved in 10 wt. % nitric acid (10 ml of nitric acid completed by 90 ml of deionized water). The solution is refluxed under stirring at 600 rpm and temperature at 80 °C for 12 h.

### 2.2: Preparation of MnO<sub>2</sub> / modified MWCNTs nanocomposite

Weight 0.1 g from modified MWCNTs was added in 25 ml from deionized water by ultrasonic vibration for 2 h. and was added 0.3 g KMnO<sub>4</sub> into the above suspension, and the mixed solution was stirred by a magnetic rod for 2 h. Next that the mixed solution was transferred to a 30 mL, Teflon-lined, stainless steel autoclave. The autoclave was closed and put in an electric oven at 150°C for 6 h and then naturally cooled to room temperature. Next the hydrothermal treatment, the resultant samples (MnO<sub>2</sub>/MWCNTs) were collected by filtration and washed with deionized water. MnO<sub>2</sub>/MWCNTs nanocomposite were finally dried in an oven at 100°C for 12 h.

### 2.3 :Preparation of MnO<sub>2</sub>/ MWCNTs /PVA nanocomposite thin film

The dried MnO<sub>2</sub>/ MWCNTs was added into three different amounts of PVA solutions (0.5, 1, 1.5 wt. %) and stirred at 80°C until a homogenous solution was obtained. The solution was ultrasonicated for 5 h. Then, the solution was poured into Petri dishes, followed by solvent evaporation at room temperature to form MnO<sub>2</sub>/modified MWCNTs/PVA thin films.

### 2.4 : Characterization

The crystallographic information of the acid-treated MWCNTs and the MnO<sub>2</sub>/ MWCNTs nanocomposite were characterized by X-ray diffraction [XRD], using (Philips PW 1370), with Cu, K $\alpha$ , ( $\lambda = 0.154$  nm). Transmission electron microscope (TEM, JEOL JEM-3010, 300 kv) was used to characterize the morphology of the modified MWCNTs and MnO<sub>2</sub>/MWCNTs nanocomposite. The chemical structures of the MWCNTs and the MnO<sub>2</sub>/MWCNTs nanocomposite were characterized by Fourier transform infrared (FT-IR) spectroscopy using the device (Thermo Nicolet, FT-IR and NEXUS) in the range of 4000–400 cm<sup>-1</sup>. UV-Vis absorption spectra of PVA pure and MnO<sub>2</sub> / MWCNTs / PVA nanocomposite thin films, were measured using UV-Vis spectrometer (6100 Jusco, Japan). At room temperature the electrical properties were measured by using the device (Hioki, LCR Hitester 3532-50). The frequency dependence of electrical properties for as-prepared samples were measured on the frequency range (100Hz-6MHz).

## 3. Results and discussion

### 3.1: XRD

XRD patterns of the MWCNTs, modified MWCNTs and MnO<sub>2</sub>/ MWCNTs nanocomposite are shown in Fig.1. XRD pattern of the MWCNTs shows three diffraction peaks at 2 $\theta$  values of 25.59°, 43.13° and 77.74° which can be indexed as the (002), (101), and (110) planes of graphite carbon [14]. The very sharp peak corresponding to the structure of MWCNTs, modified MWCNTs at 25.59° of 2 $\theta$  becomes very weak at 26.42° of 2 $\theta$  in the MnO<sub>2</sub>/ MWCNTs nanocomposite, also the peak at 43.13° of 2 $\theta$  in the MWCNTs shifted to 44.62° and becomes thinner in the MnO<sub>2</sub>/ MWCNTs nanocomposite. The new sharp diffraction peak at 9.29° of 2 $\theta$  in the MnO<sub>2</sub>/ MWCNTs nanocomposite can be perfectly indexed as (001) planes of MnO<sub>2</sub> [15-16], after the deposition of MnO<sub>2</sub>, indicating that the surfaces of MWCNTs are uniformly covered by MnO<sub>2</sub>. The crystalline structure of MnO<sub>2</sub> are composed of one Mn atom surrounded by six O atoms to form an octahedron. The MnO<sub>6</sub>

octahedral subunits share vertices and edges to form crystalline tunnel structures by continuously linking to the neighboring subunits [17]. The crystallite size of the modified MWCNTs and MnO<sub>2</sub>/MWCNTs nanocomposite was calculated using Scherrer's from this Eq. [18]:

$$D = \frac{K\lambda}{\beta \cos \theta}$$

Where: the crystal grain size is D (nm), the Scherrer constant is K (0.89), the X-ray wavelength is  $\lambda$  (0.154056 nm) for Cu K $\alpha$ , the full width at half maximum intensity (FWHM) is  $\beta$  in radian and the Bragg angle in degree is  $\theta^\circ$ . The calculations reveal that the crystal grain size of the modified MWCNTs and MnO<sub>2</sub>/MWCNTs nanocomposite are 7.22nm and 9.96 nm respectively.

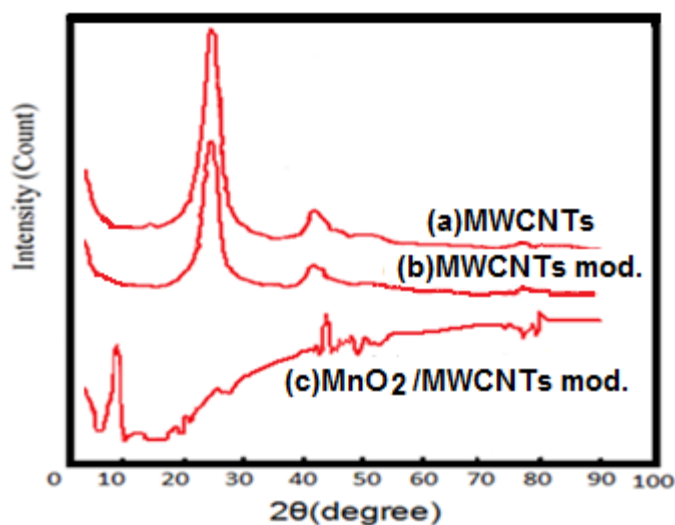


**Fig. 1: XRD patterns of the (a) MWCNTs and (b) modified MWCNTs and (c) MnO<sub>2</sub> / MWCNTs nanocomposite .**

### 3.2: TEM

The TEM images of modified MWCNTs and MnO<sub>2</sub>/MWCNTs nanocomposite are shown in Fig.2 (a) and (b) respectively. The average diameter of nanotubes modified MWCNTs is about 10.11 nm. Which is in agreement with results obtained for crystallite sizes in the XRD study. Also, fig.2 (b) indicates that MnO<sub>2</sub> inside the modified MWCNTs in nanocomposite with an average diameter of about 4 nm. These images conform the interaction between modified MWCNTs and MnO<sub>2</sub> nanocomposite. Therefore the nanotubes from TEM images for modified MWCNTs and MnO<sub>2</sub>/MWCNTs nanocomposite are of high purity, with uniform diameter distribution, and contain no deformity in the structure.

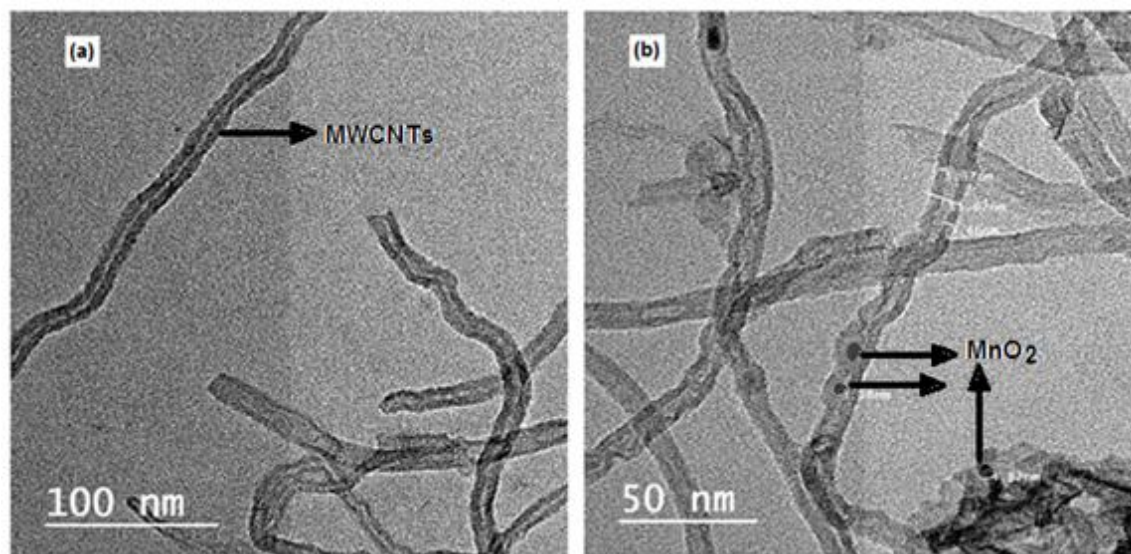


**Fig. 2: TEM of (a) modified MWCNTs and (b) MnO<sub>2</sub> / MWCNTs nanocomposite .**

### 3.3: FT-IR Spectroscopy

Fig.3 shows FT-IR spectra of MWCNTs ,modified MWCNTs and MnO<sub>2</sub>/MWCNTs nanocomposite .It can be noticed that, a broad absorption band at 3430 cm<sup>-1</sup> attributed to O-H stretching which may be due to ambient atmospheric moisture[19]. Also it can be noticed that this band increase in the broadening and shifted at 3425 cm<sup>-1</sup>, 3420 cm<sup>-1</sup> in case of modified MWCNTs and MnO<sub>2</sub>/MWCNTs nanocomposite as shown in table (1). The weak band at 2920 cm<sup>-1</sup> in MWCNTs shifted to 2915 cm<sup>-1</sup> and 2910 cm<sup>-1</sup> for modified MWCNTs and MnO<sub>2</sub>/ MWCNTs nanocomposite is assigned to C-H bending, stretching [20]. The new weak band appeared at 2375 and 2347cm<sup>-1</sup> in the spectra of modified MWCNTs and MnO<sub>2</sub>/ MWCNTs nanocomposite disappeared in the spectrum of the MWCNTs is the asymmetric and symmetric CH<sub>2</sub> stretching [21].

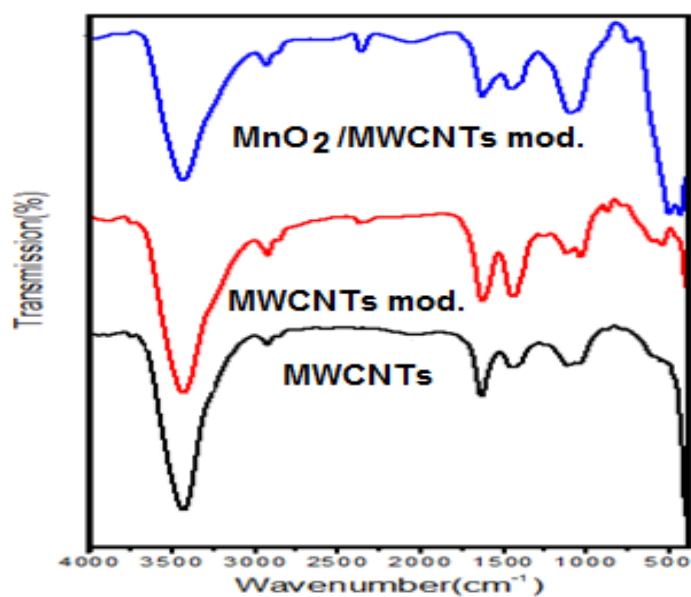


**Fig. 3: FT-IR spectra of the MWCNTs , modified MWCNTs and MnO<sub>2</sub> / MWCNTs nanocomposite .**

Also, the medium band at  $1630\text{ cm}^{-1}$  in the spectrum of the MWCNTs shifted at  $1625\text{ cm}^{-1}$  in the spectra of modified MWCNTs and  $\text{MnO}_2/\text{MWCNTs}$  nanocomposite is assigned to conjugated C=C stretching. This finding confirms the hexagonal structure of the MWCNTs [22]. The medium band at  $1440\text{ cm}^{-1}$  in the spectrum of the MWCNTs shifted at  $1430\text{ cm}^{-1}$  in the spectrum of the  $\text{MnO}_2/\text{MWCNTs}$  nanocomposite is assigned to O-H stretching [23]. The medium band at  $1050\text{ cm}^{-1}$  in the spectrum of the MWCNTs shifted at  $1097\text{ cm}^{-1}$  in the spectrum of the  $\text{MnO}_2/\text{MWCNTs}$  nanocomposite corresponding to C-O stretching [23]. The presence of these functional groups implies that the as-received MWCNTs already have several functional groups that were introduced during the proprietary synthesis and/or purification processes. The new peak at  $500\text{ cm}^{-1}$  in the spectrum of  $\text{MnO}_2/\text{MWCNTs}$  nanocomposite can be assigned to the Mn-O and Mn-O-Mn vibrations [24], which is related to the vibration of  $\text{MnO}_6$  octahedron. The functionalization of MWCNTs can increase the active sites, which contribute to the combination between  $\text{MnO}_2$  and MWCNTs in the preparation process of  $\text{MnO}_2/\text{MWCNTs}$  material.

**Table 1. Peak positions ( $\text{cm}^{-1}$ ) and assignment of infrared spectra of investigated various MWCNTs, modified MWCNTs and  $\text{MnO}_2/\text{MWCNTs}$  nanocomposite.**

Wavenumber [ $\text{cm}^{-1}$ ] MWCNTs	Wavenumber [ $\text{cm}^{-1}$ ] modified MWCNTs	Wavenumber [ $\text{cm}^{-1}$ ] $\text{MnO}_2/\text{MWCNTs}$	relative intensity	Band assignments	Reference
3430	3425	3420	Broad	attributed to O-H stretching	[19]
2920	2915	2910	weak	C-H bending, stretching	[20]
---	2375	2347	weak	for the asymmetric and symmetric CH <sub>2</sub> stretching	[21]
1630	1625	1625	medium	assigned to conjugated C=C stretching	[22]
1440	1444	1430	medium	O-H stretching	[23]
1050	1027	1097	medium	corresponding to C-O stretching	[23]
-----	-----	500	medium	Mn-O and Mn-O-Mn vibrations	[24]

### 3.4 : Optical Measurements

Fig.4. shows UV-Vis absorption spectra of PVA pure and (0.5,1 and1.5%) of  $\text{MnO}_2/\text{MWCNTs}/\text{PVA}$  nanocomposites. The measurements of absorption spectra were carried out at room temperature for visible wavelength ranging from 200 nm to 800 nm. The absorption spectrum of pure PVA has two absorbance bands at 276 and 340 nm. The first band is assigned to the electronic transitions  $\pi \rightarrow \pi^*$  [25] and shifted at 268 nm for the spectrum of 1.5%  $\text{MnO}_2/\text{MWCNTs}/\text{PVA}$  nanocomposite. The second band assigned as  $n \rightarrow \pi^*$ , the absorption intensity of these bands of the  $\text{MnO}_2/\text{MWCNTs}/\text{PVA}$  nanocomposite films increases with

increasing  $\text{MnO}_2$  wt% in the samples and shifted to higher wavelength . As can be seen, the absorbance is unaffected in the UV range (400- 800 nm wavelength) with exposed time and remains unchanged.

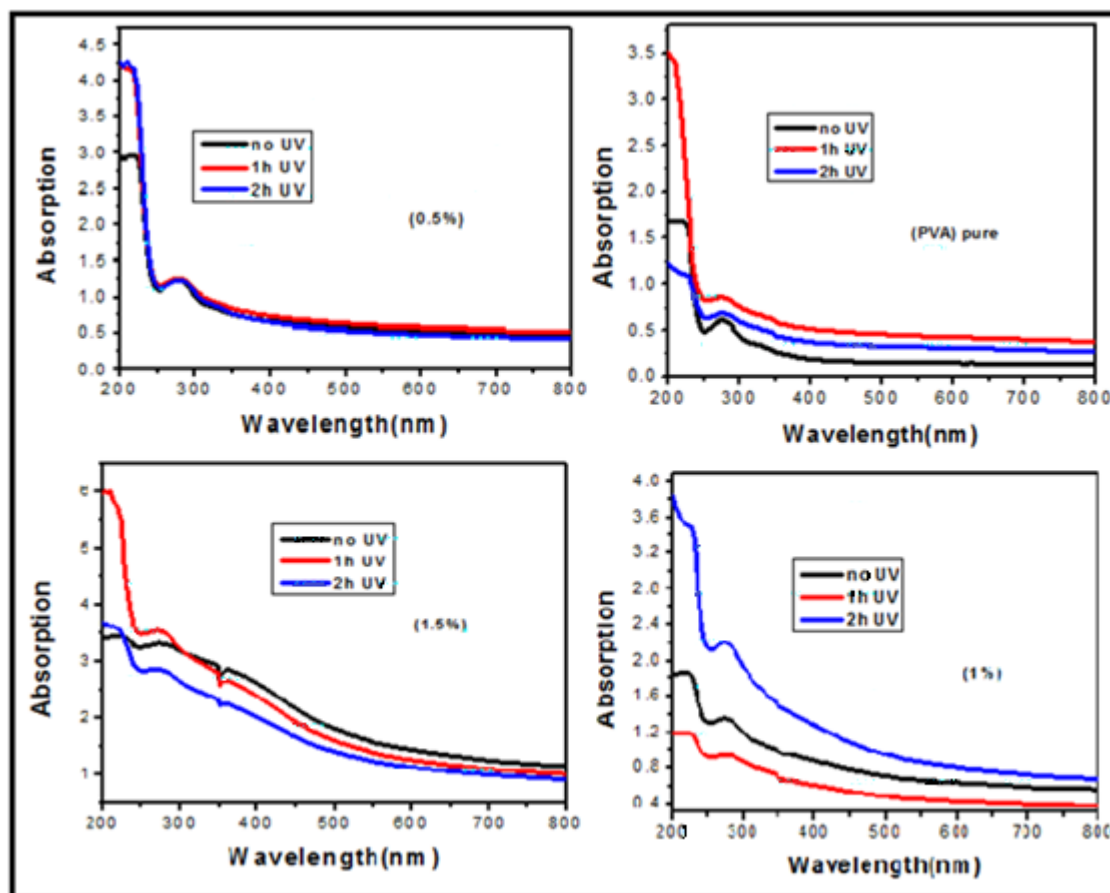


**Fig. 4: UV-Vis absorption spectra of PVA pure , 0.5,1 and 1.5 %  $\text{MnO}_2$  / MWCNTs / nanocomposite thin films**

The optical band gap of the samples before and after exposing UV-VIS radiation were calculated and listed in table (2). It can be noticed that, the value of  $E_g$  in case of PVA pure thin film equal to 3.257 eV at room temperature and in agreement with [26] also it decreases with increasing exposing UV-irradiation. The absorption spectra shifted at different exposing time, indicated the sensitivity to UV radiation .

**Table 2: the optical band gap of the samples before and after exposing UV-irradiation**

material	0 hour (Eg/eV)	1 hour (Eg/eV)	2 hour (Eg/eV)
PVA pure thin film	3.257	2.750	2.633
(0.5%) $\text{MnO}_2$ /MWCNTs/PVA nanocomposite thin film	2.750	2.660	2.578
(1%) $\text{MnO}_2$ /MWCNTs/PVA nanocomposite thin film	2.475	2.013	1.980
(1.5%) $\text{MnO}_2$ /MWCNTs/PVA nanocomposite thin film	2.013	1.743	1.706

### 3.5: Electrical Properties:

The most important basic dielectric parameters, which play a major role in the determination of material properties, are the dielectric constant ( $\epsilon'$ ), dielectric loss ( $\epsilon''$ ), conductivity ( $\sigma$ ) and resistivity ( $\rho$ ) of PVA pure and MnO<sub>2</sub> /MWCNTs/ PVA nanocomposite thin film with different concentration according to different frequency and exposing time of UV radiation were shown in (Fig.5-8). The results showed that the conductivity increases with increasing frequency and UV exposing time of the MnO<sub>2</sub> / MWCNTs / PVA nanocomposite thin films as shown in table (3).

**Table 3: Data of  $\epsilon'$ ,  $\epsilon''$ ,  $\sigma$  ( $\Omega \cdot m^{-1}$ ) and  $\rho$  ( $\Omega \cdot m$ ) for the prepared compounds at different time of exposure to UV, 100 Hz and room temperature.**

film type	Time of UV-radiation	$\epsilon'$	$\epsilon''$	$\sigma$ ( $\Omega \cdot m^{-1}$ )	$\rho$ ( $\Omega \cdot m$ )
PVA pure	0h	2.25	16.92	--18.83	7.23
	1 h	181.13	19.59	--15.96	8.09
	2 h	70.9	159.03	--17.35	8.51
0.5%MnO <sub>2</sub> /MWCNTs/PVA nanocomposite	0h	50.3 2	16.91	-16.67	9.22
	1 h	35.29	223.22	-16.50	8.24
	2 h	2.96	19.54	-15.96	8.76
1%MnO <sub>2</sub> /MWCNTs/PVA nanocomposite	0h	9.22	27.6	-16.9	10.07
	1 h	42.03	168	-17.5	9.39
	2 h	9.87	18.79	-17.3	9.84
1.5%MnO <sub>2</sub> /MWCNTs/PVA nanocomposite	0h	5.11	50.34	-17.27	9.58
	1 h	5.13	70.12	-16.96	9.84
	2 h	160	85.36	-16.66	10.42

This means that, the resistivity of the nanocomposite thin films decreases by introducing a conductive network into the polymer matrix which improves the conductivity. This may be due to the larger surface area of MWCNTs that serve as a conducting bridge, connecting conducting domains and increasing the effective percolation. Also, interaction of UV radiation with nanocomposite particles which affect the interaction between them. This advantages obtained, is the possibility of improve the charge transport properties of the MnO<sub>2</sub> / MWCNTs / PVA nanocomposite thin films.

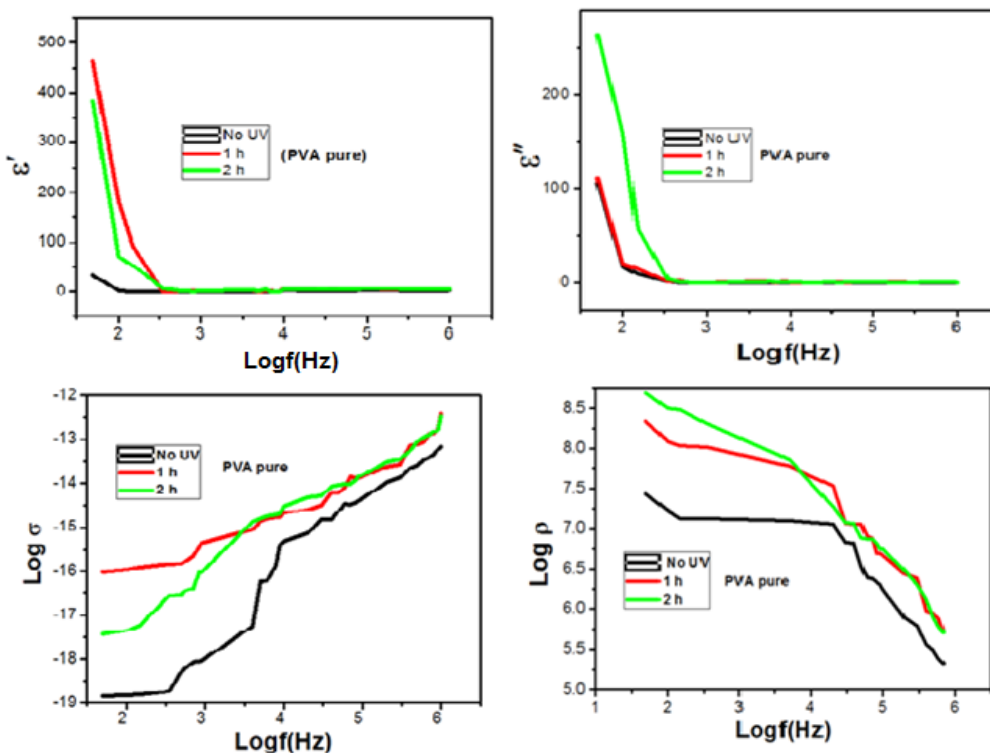


Fig. 5 : Variation of  $\epsilon'$ ,  $\epsilon''$ ,  $\text{Log} \sigma$  and  $\text{Log} \rho$  of PVA pure thin film.

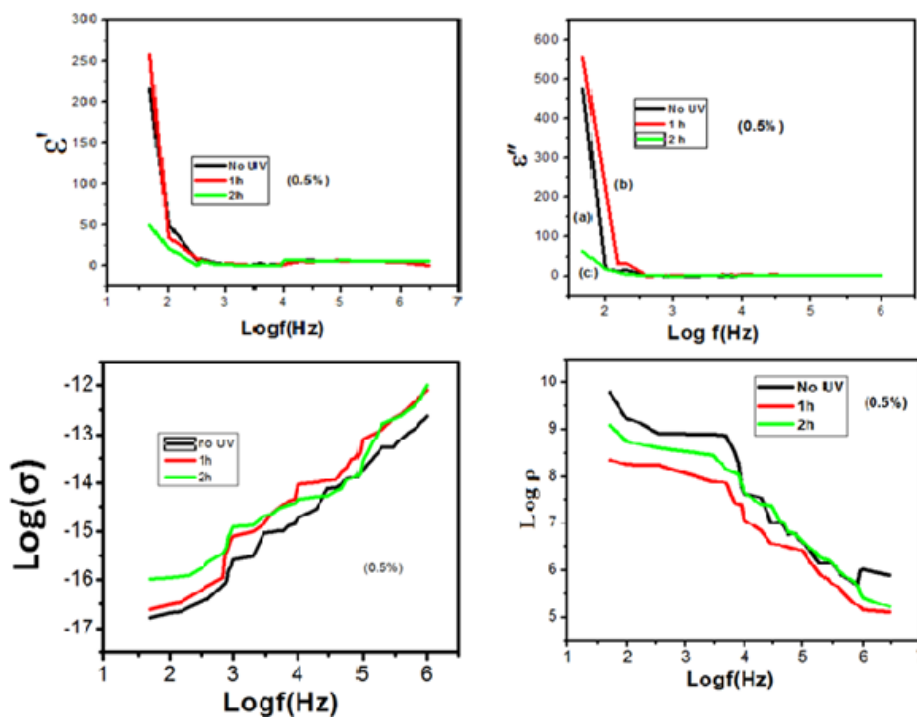


Fig. 6 : Variation of  $\epsilon'$ ,  $\epsilon''$ ,  $\text{Log} \sigma$  and  $\text{Log} \rho$  of MnO<sub>2</sub> / MWCNTs nanocomposite/ PVA thin film with concentration 0.5% .

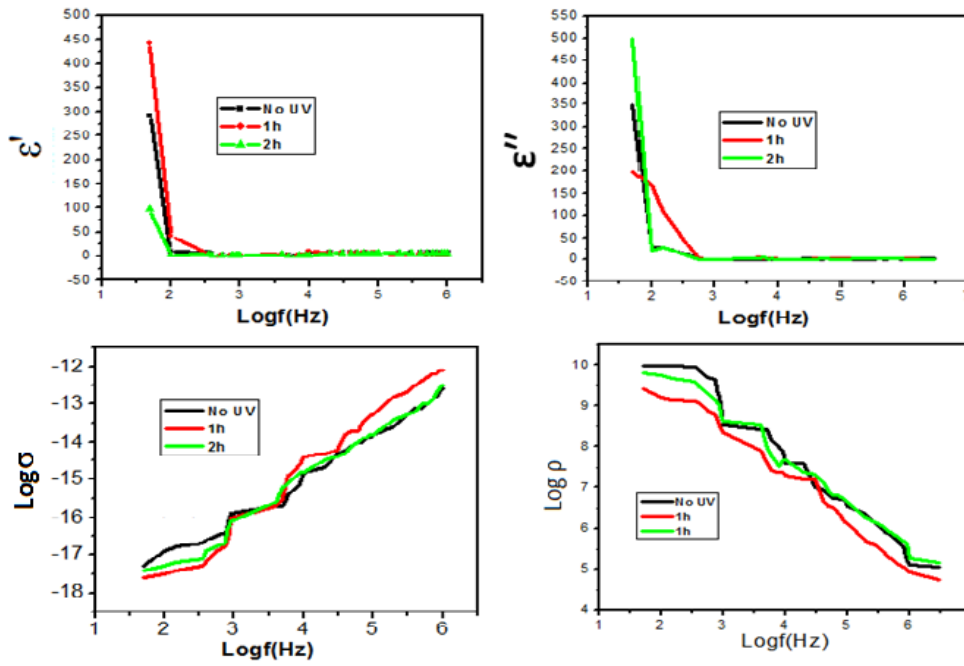


Figure 7 : Variation of  $\epsilon'$ ,  $\epsilon''$ ,  $\text{Log}\sigma$  and  $\text{Log}\rho$  of 1%  $\text{MnO}_2$  / MWCNTs / PVA nanocomposite thin film .

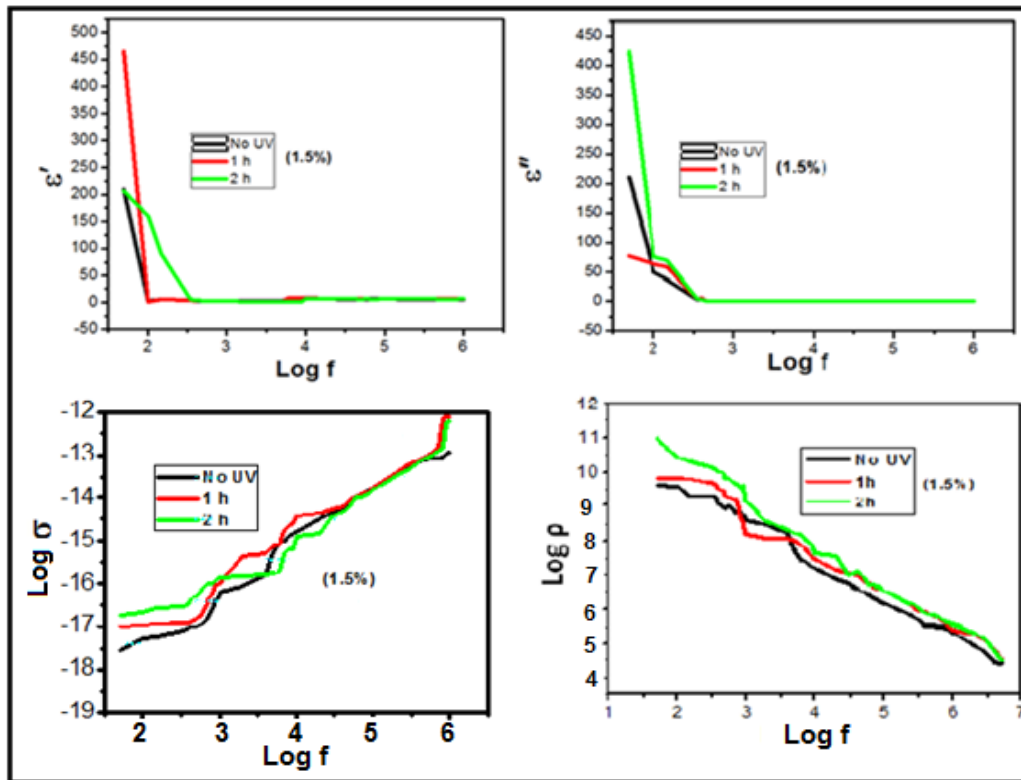


Fig. 8 : Variation of  $\epsilon'$ ,  $\epsilon''$ ,  $\text{Log}\sigma$  and  $\text{Log}\rho$  of 1.5%  $\text{MnO}_2$  / MWCNTs nanocomposite/PVA nanocomposite thin film .

#### 4. Conclusions

$\text{MnO}_2$ / MWCNTs nanocomposite were successfully by hydrothermal method with different concentration of  $\text{MnO}_2$  using a surface oxidation reaction between  $\text{KMnO}_4$  and MWCNTs. Nanocomposite

were characterized by X-ray diffraction(XRD) and TEM analysis and images confirmed homogeneous dispersion of MnO<sub>2</sub>/ MWCNTs nanocomposite. The infrared absorption spectrum indicates the presence of conjugated C=C stretching (carbon double bonds), which confirms the safety of the hexagonal structure of the MWCNTs . Sensitivity to UV –irradiation were studied on the optical and electrical properties of the MnO<sub>2</sub>/ MWCNTs nanocomposite thin films prepared samples have been evaluated . The band gap value were varied due to change in its grain size and time of UV- irradiation. Also, Dielectric properties were affected by radiation. Electrical behavior showed semiconducting properties and sensitivity to UV –radiation. The results indicate the possibility of using MnO<sub>2</sub> /MWCNTs nanocomposite as UV detector.

## References

- [1] Liu DW, Zhang QF, Xiao P, Garcia BB, Guo Q, Champion R, Cao GZ. *Chem Mater.* 2008;20:1376–1380.
- [2] Masciangioli T, Zhang W-X (2003) Environmental technologies at the nanoscale .*Environ Sci Technol* 102A–108A.
- [3] Li WN, Yuan JK, Gomez-Mower S, Xu LP, Sithambaram S, Aindow M, Suib SL. *Adv Funct Mater.* 2006;16:1247–1253.
- [4] Yan JA, Khoo E, Sumboja A, Lee PS. *ACS Nano.* 2010;4:4247–4255.
- [5] Li ZQ, Ding Y, Xiong YJ, Yang Q, Xie Y. *Chem Commun.* 2005;7:918–920.
- [6] Reddy ALM, Shajjumon MM, Gowda SR, Ajayan M. *Nano Lett.* 2009;9:1002–1006.
- [7] Chen S, Zhu JW, Han QF, Zheng ZJ, Yang Y, Wang X. *Cryst. Growth Des.* 2009;9:4356–4361.
- [8] Hou Y, Cheng YW, Hobson T, Liu J. *Nano Lett.* 2010;10:2727–2733.
- [9] Ko JM, Kim KM. *Mater Chem Phy.* 2009;114:837–841.
- [10] Wang YH, Liu H, Sun XL, Zhitomirsky I. 2009;61:1079–1082.
- [11] Raymundo-Pinero E, Khomenko K, Frackowiak E, Beguin F. *J Electrochem Soc.* 2005;152:A229–A235.
- [12] Yan J, Fan ZJ, Wei T, Cheng J, Shao B, Wang K, Song LP, Zhang ML. *J Power Sources.* 2009;194:1202–1207.
- [13] M. Pang, G. Long, S. Jiang, Y. Ji, W. Han, B. Wang, X. Liu, Y. Xi, *Mater. Sci. Engin. B*, 194 (2015) 41.
- [14] H.J. Wang, L.L. Zhu, S. Peng, F. Peng, H. Yu, J. Yang, *Renew. Energy*37(2012)192-196.
- [15] Q.T. Qu, L. Li, S. Tian, W.L. Guo, Y.P. Wu, R. Holze, *J. Power Sources* 195 (2010) 2789–2794.
- [16] Y.P. Lin, C.B. Tsai, W.H. Ho, N.L. Wu, *Mater. Chem. Phys.* 130 (2011)367–372.
- [17] Hamid Reza Naderi , Mohammad Reza Ganjali and Parviz Norouzi, *Int. J. Electrochem. Sci.*, 11 (2016) 4267 – 4282.
- [18] Ahmad Monshi, Mohammad Reza Foroughi, Mohammad Reza Monshi . *World Journal of Nano Science and Engineering*,2, (2012), 154-160 .
- [19] F. Aviles, J.V. Cauich-Rodriguez, L. Moo-Tah, A. May-Pat, R. Vargas-Coronado, *Carbon* 47 (2009) 2970–2975.

[20] R. Yudianti ,H. Onggo, Y. Saito, T. Iwata, and J .-I.Azuma .Open Materials Science Journal , 5, (2011),242–247.

[21] F .Avilés, J.V. Cauich- Rodríguez, L. Moo-Tah, A. May-Pat, & R.Vargas-Coronado, 47(2009)2970-2975.

[22] R. Yudianti, H. Onggo, Y. Saito, T. Iwata, and J.-I.Azuma. Open Materials Science Journal ,vol.5, (2011),pp.242–247.

[23] F. Avilés, J.V. Cauich-Rodríguez, J.A .Rodríguez-Gonzalez, A. May-Pat Express Polymer Letters Vol.5, No.9 (2011) 766–776.

[24] X.F. Xie, L. Gao, Carbon 45 (2007) 2365–2373.

[25] A. M. Shehap, Egypt. J. Splids, 1 (2008), 75-91.

[26] A. Mang, K. Reimann and Rubenacke St, Solid State Commun, 94(1995) 251-254.